Prediction of jet Mach and Reynolds numbers from acoustic measurements

Juan José Peña Fernández and Jörn Sesterhenn

Institut für Strömungsmechanik und Technische Akustik, 10623 Berlin, Deutschland, Email: fernand@tnt.tu-berlin.de

Introduction

The prediction of the jet Mach and Reynolds numbers from acoustic measurements is of great interest, for example, to develop new strategies for volcanic monitoring or to develop new models of how much ash is released into the atmosphere during a specific volcanic eruption to improve the air traffic in volcanic areas.

There are around 500 active volcanoes in the world, and some of them are a hazard for several millions of people all around the globe. A new volcanic monitoring system based on acoustic measurements through which the main parameters of the volcanic jets are predicted in real time would definitely help the existing volcanic monitoring systems, being a very sensitive method that can predict accurately the main parameters of volcanic jets and it would be a cost-effective option.

With knowledge about the governing parameters of volcanic jets and additional information about the characteristic particle density and particle size distribution of the eruptions of a specific volcano, we are a step closer to develop new models of how much ash is released into the atmosphere during a specific volcanic eruption. With this information, the methods to predict the ash distribution in the atmosphere during and after an eruption will be more reliable and the air traffic in the volcanic regions will be more efficient and safer.

Supersonic jet noise has been investigated since the 1950s for the continuous jet, [1]. The components of supersonic jet noise, together with their generation mechanisms are clearly summarised in [2]: turbulent mixing noise (TMN), broadband shock noise (BBSN) and screech tones. Recently, the main acoustic sources of the starting jet were reported in [3]; the acoustic radiated by the vortex ring and the compression wave were added to the three classical noise sources of the continuous jet.

The main objective of this study is to predict the Reynolds and Mach numbers of supersonic jets from acoustic measurements using a single microphone and as few additional information about the system as possible.

This rest of this article is structured as follows: the next section describes the methods used in this study, followed by the discussion of the main results of this study: first we focus on the prediction of the Reynolds number, then on the Mach number and finally the application of this methods to laboratory experiments and fieldwork measurements on real volcanoes. The last section completes this work by drawing the conclusions.

Methods

A combination of numerical and experimental approaches were used in this study to have a global overview of the system, using the advantages of every method.

Direct numerical simulations of starting jets were performed as reported in [4]. The generation of the main supersonic jet noise sources was investigated and the relationships from the literature between the peak Strouhal numbers of the different sources with the governing parameters were confirmed. The analysis of these numerical simulations provided us deeper knowledge about the noise generation mechanisms in the supersonic starting jet.

Experiments of supersonic (continuous and starting) jets were performed in the laboratory with a reservoir to ambient pressure ratio in the range $1.9 - 6$. The diameter of the nozzle was 10 mm. The temperature of both the reservoir (T_{0r}) and the ambient (T_∞) was 298 K. The diameter of the reservoir with which the starting jets were generated was the same as the nozzle diameter and the ratio reservoir length to diameter (L/D) was in the range $2-8$. We measured the acoustic radiated by these jets in the anechoic chamber of the Berlin Institute of Technology. We also used the high-speed Schlieren photography method to compare the flow field generated by the different parameter sets. This experimental parameter analysis was designed to evaluate the changes in the acoustic field for specific conditions.

During a fieldwork campaign on Stromboli (Italy) in October 2017, we measured the acoustic radiated by the 4 active vents of the volcano during approximately 7 hours a day for 7 days. Approximately 500 events were recorded with a large spectrum of eruption features. This fieldwork campaign was programmed to apply the methods developed and estimate the main parameters of volcanic jets.

Results and discussion

In this section we discuss the results of this study starting with the prediction of the Reynolds number, followed by the Mach number.

Prediction of the Reynolds number

Turbulent mixing noise is the only jet noise component where turbulence is exclusively involved. Since the Reynolds number is used to characterise turbulence in flows, the properties of the turbulent mixing noise are appropriate to predict the Reynolds number.

By increasing the Reynolds number of the jet, the relative size of the Kolmogorov scale to the nozzle diameter

decreases, [5]. Moreover, the peak Strouhal number of the fine-scale turbulent mixing noise increases when increasing the Reynolds number, as reported in [6]. Taking into account the two previous results, we can deduce that an increase in the Reynolds number leads to smaller vortices, which turns into a higher dominant frequency for the noise related to turbulence. A limit of Re approximately 400 000 was estimated in [7] as the end of the 'low Reynolds number effect' range. This would mean that for larger Reynolds numbers, the acoustic properties of the fine-scale turbulent mixing noise do not change. There is no agreement in the community about this number and future work is planned.
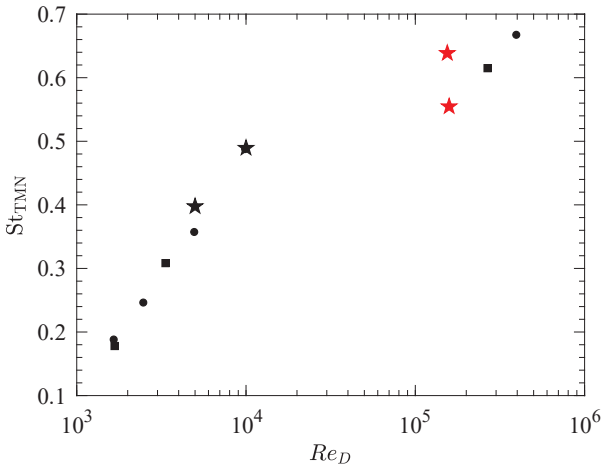

Figure 1: Variation with the Reynolds number of the Strouhal number of the fine-scale turbulent mixing noise (St_{TMN}). The acoustic was measured at 90° with respect to the jet axis in all cases. ● corresponds to a jet Mach number of 0.9 and ■ to a jet Mach number of 0.6, both from [6]. The two black stars correspond to numerical simulations from [4] with a Mach number of 1.48 for Reynolds numbers of 5 000 and 10 000. The red stars correspond to experiments from this study with a Mach number of 0.89 and 0.95.

Figure 1 shows the comparison of experimental and numerical data of the evolution with the Reynolds number of the Strouhal number for the fine-scale turbulent mixing noise. The two black stars correspond to direct numerical simulations reported in [4]; the two red stars correspond to experiments from this study. There is a clear correlation between these two variables that we use to predict the Reynolds number when measuring the dominant frequency of the fine-scale turbulent mixing noise.

Prediction of the Mach number

In this subsection we discuss the prediction of the Mach number. We use first the acoustic radiated by the broadband shock noise, followed by the screech tones.

The shock-cell spacing (L_s) is the proper length to scale supersonic phenomena as proposed in [8]; the Strouhal number of the broadband shock noise peak frequency St_{BBSN} based on the shock-cell spacing and the convective velocity $u_c = 0.7u_j$ was reported to be a constant value around one.

$$St_{BBSN} = \frac{f_{BBSN} L_s}{u_c} \approx 1 \qquad (1)$$

Based on this and the knowledge of how the shock-cell spacing changes with the fully expanded Mach number, see [9]:

$$\frac{L_s}{D} = \pi\, \sigma_1 \sqrt{M_j^2 - 1}\, \frac{D_j}{D}$$

where σ_1 is the first root of the zero-order Bessel function and D_j is the fully expanded diameter of the flow.
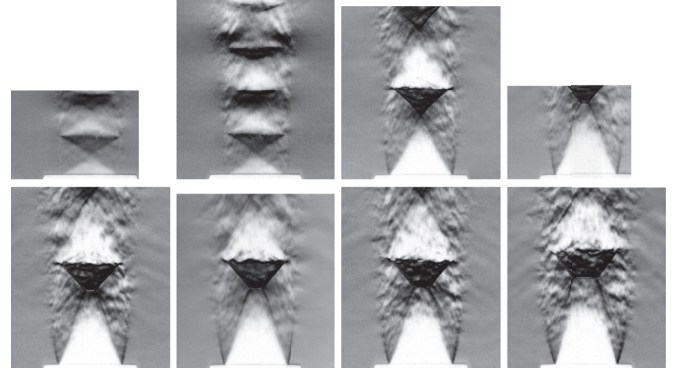

Figure 2: Effect of the Mach number on the shock-cell spacing. The Mach numbers of the different jets from left to right and top to bottom are: 1.09; 1.10; 1.38; 1.43; 1.48; 1.50; 1.51 and 1.56. The high-speed Schlieren method was used to visualise the flow.

We found a relationship between the Helmholtz number of the broadband shock noise peak frequency H_{BBSN} and the fully expanded Mach number M_j:

$$H_{BBSN} = \frac{f_{BBSN} D}{c_\infty} = \frac{\sigma_1}{\pi \sqrt{M_j^2 - 1}} \frac{D}{D_j} \frac{c_j}{c_\infty} \qquad (2)$$

where D_j/D and c_j/c_∞ are a known function of the Mach number.

Our numerical simulations and laboratory experiments were performed with isothermal conditions ($T_{0r}/T_\infty = 1$) and a convergent nozzle ($M_d = 1$). This model is represented in figure 3 as the solid black line.

The only information needed to use this model is the nozzle diameter, the ambient speed of sound and acoustic measurements of the broadband shock noise at 90°, because the broadband shock noise shows a Doppler shift with the jet angle.

Using the screech tone to predict the Mach number has the advantage that the peak frequency is very easy to identify and it does not show any Doppler shift, so there is no restriction on the angle for which the acoustic is measured.

There are several ways in the literature to model the screech frequency with the Mach number. We adapted the model reported in [10] as follows:
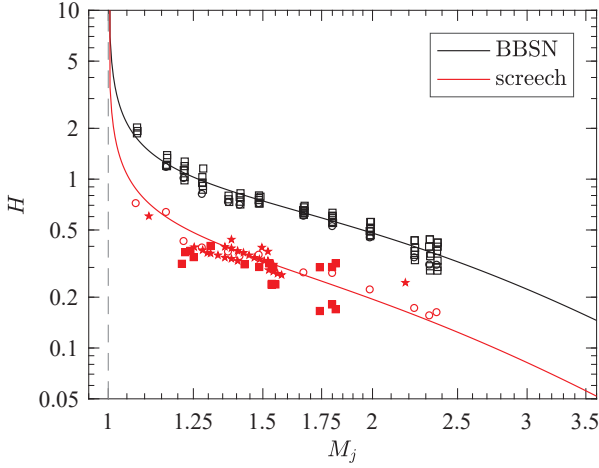
Figure 3: Variation of the Helmholtz number with the Mach number. The empty symbols correspond to experimental results from [8]. The black line corresponds to the model of the current study to predict the broadband shock noise. The red line corresponds to the model of the current study to predict the screech tone. The filled red stars correspond to experimental data from the current study measured on continuous jets and the filled red squares correspond to experimental data from the current study on starting jets.

$$H_s = \frac{\frac{c_j}{c_\infty}}{\frac{D_j}{D}} \frac{0.6 M_j}{\sqrt{M_j^2 - 1}} \left(1 + \frac{0.7 M_j}{\sqrt{1 + \frac{\gamma - 1}{2} M_j^2}} \sqrt{\frac{T_\infty}{T_{0r}}} \right)^{-1} \quad (3)$$

where H_s is the screech Helmholtz number. This model is represented in figure 3 as the solid red line.

As opposed to the method using the broadband shock noise, the acoustic measurements do not need to be at 90° with respect to the jet axis, because the screech tones do not show Doppler shift. This means the only information that we need to predict the Mach number using the screech tone is the nozzle diameter, the speed of sound for ambient conditions and the acoustic of one microphone in the side-forward arc, where the screech tone is radiated.

Application to laboratory jets

In this section, we apply the methods developed in the previous section to the experiments performed in the laboratory under controlled conditions.

Figure 4 shows the sound pressure level as a function of the non-dimensional time ($t\, U/D$) and the Strouhal number. The complex Morlet wavelet was used to compute the time-dependent spectrum. The reservoir length to diameter ratio of this example was $L/D = 2$. The initial pressure ratio was $p_{0r}/p_\infty = 80$. We can identify the acoustic footprint of the main features of the starting jet in the wavelet diagram, based on the orders of magnitude of the size and velocities of the different elements as well as their behaviour. This way we can state that the first compression wave shows the typical lobe in the wavelet diagram, wider for low Strouhal numbers

and finer for higher Strouhal numbers due to the higher accuracy of the wavelet transformation to locate events with smaller wavelengths. The same way, the size of the vortex ring is the same order of magnitude than the nozzle diameter, but its velocity is as low as two orders of magnitude less than the characteristic velocity U (taken as the fully expanded velocity of an infinite reservoir with $p_{0r}/p_\infty = 80$). The footprint of the trailing jet vanishes much faster than that of the vortex ring, with a peak frequency of about $St_{BBSN} \approx 0.1$.
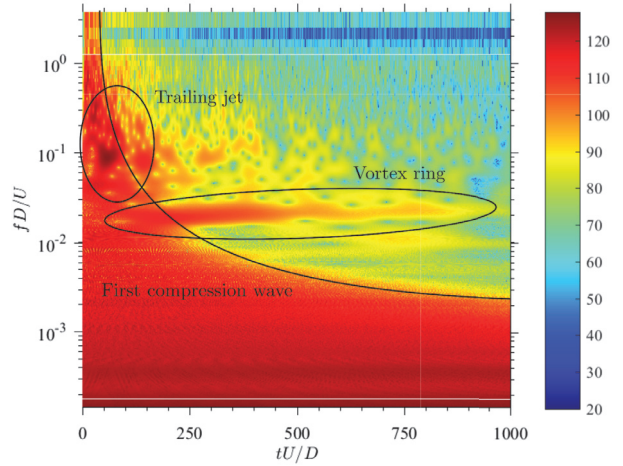

Figure 4: Evolution of the sound pressure level with the non-dimensional time and the Strouhal number. The units of the colour-scale are [dB]. The complex Morlet wavelet was used to compute the time-dependent spectrum.

Building the broadband shock noise peak Helmholtz number out of the peak Strouhal number we get $H_{BBSN} = 0.3180$. This leads to a Mach number of $M_j = 1.6$, which is a realistic value for this setup. For such a small reservoir, the time of discharge was too small to generate screech tones, so we were not able to have a prediction based on the screech tone.

Application to volcanic jets

In this subsection we apply the methods developed in this study to real volcanic eruptions.

In this case, the conditions are not so well known as in laboratory. With an estimated vent diameter of $D = 3$m based on aerial photography with drones and an ambient temperature of $T_\infty = 290$K, we apply the previous methods to the acoustic measurements.

We found typically the four cases shown in figure 5: (i) subsonic, (ii) short supersonic, (iii) long supersonic and (iv) multi-pulsed volcanic jets. The jet Mach numbers estimated in the fieldwork are between 1.05 and 3 and the Reynolds numbers are in the order of 10^6, which are reasonable values.

Conclusions

The link between the acoustic radiated by a supersonic jet and the jet Reynolds and Mach numbers was described as well as the expected changes in the acoustic

field with the variation of the jet Reynolds and Mach numbers.

Numerical simulations provided us a solid background about the jet noise generation mechanisms to be able to confirm the proper scaling magnitudes. Laboratory experiments allowed us to study the effects of the jet Reynolds and Mach numbers in the radiated acoustic.

Increasing the jet Reynolds number leads to smaller vortices and therefore to higher frequencies of the turbulent mixing noise. This correlation was used to predict the Reynolds number of jets from acoustic measurements.

An increase in the jet Mach number leads to an increase in the shock-cell spacing, leading to a decrease in the associated frequency for both supersonic noise sources: broadband shock noise and screech tones. We use this correlation to predict the Mach number of supersonic jets from acoustic measurements.

We applied this methods to laboratory experiments and real volcanoes to predict their main parameters with reasonable results.

References

[1] Powell, A.: On the Mechanism of Chocked Jet Noise. Proc. Phys. Soc. B. 66 (1953), 1039-1056

[2] Tam, C.K.W.: Supersonic Jet Noise. Annual Review of Fluid Mechanics 1995 27:1, 17-43

[3] Peña Fernández, J.J. and Sesterhenn, J.: Acoustic signature of an impulsively starting jet. Physics of volcanoes. 2015

[4] Peña Fernández, J.J. and Sesterhenn, J.: Compressible starting jet: pinch-off and vortex ring-trailing jet interaction. Journal of Fluid Mechanics 817 (2017), 560-589.

[5] Kolmogorov, A.: The Local Structure of Turbulence in Incompressible Viscous Fluid for Very Large Reynolds' Numbers. 1941. Doklady Akademiia Nauk SSSR, vol.30, p.301-305

[6] Bailly, C. and Bogey, C. Current understanding of jet noise-generation mechanisms from compressible large-eddy-simulations. In *Direct- and Large-Eddy-Simulation VI*. 39-48. 2006.

[7] Viswanathan, K. (2004). Aeroacoustics of hot jets. Journal of Fluid Mechanics, 516, 39-82.

[8] Norum, T.D. and Seiner, J.M. Broadband shock noise from supersonic jets. AIAA Journal, 20: 68-73, 1982

[9] Schulze, J.: Adjoint based jet-noise minimization. 2011. PhD Thesis. Technische Universität Berlin

[10] C.K.W. Tam, J.M. Seiner, J.C. Yu,: Proposed relationship between broadband shock associated noise and screech tones. Journal of Sound and Vibration, Volume 110, Issue 2, 1986, Pages 309-321.
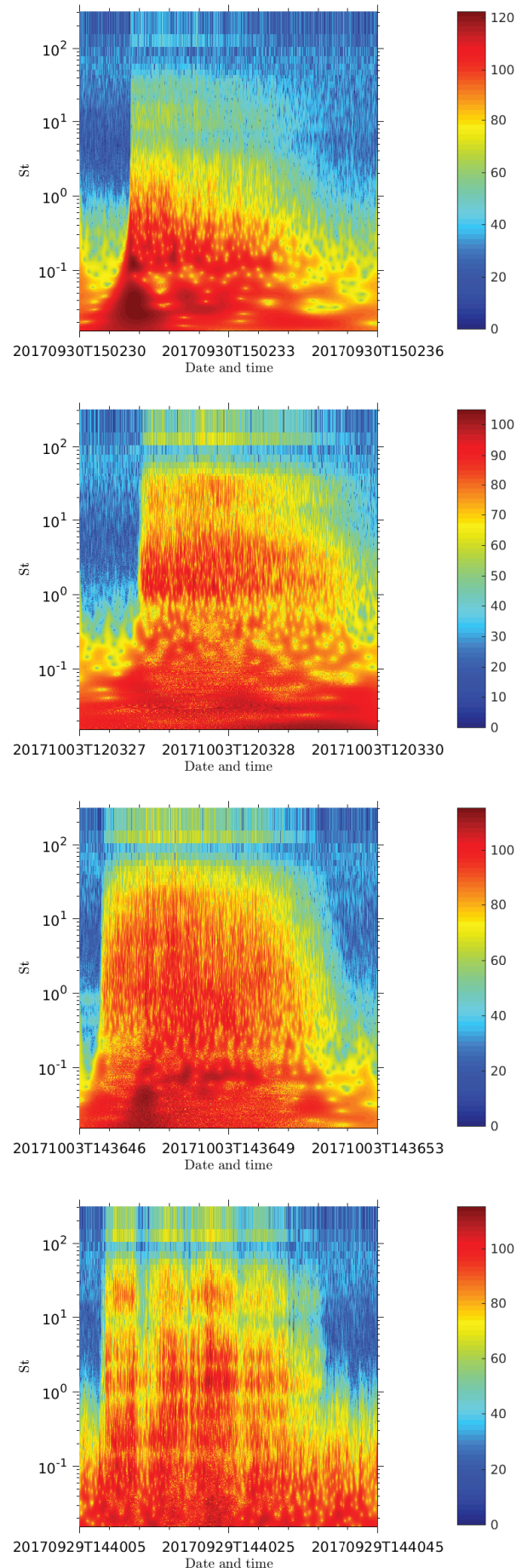
Figure 5: Evolution of the sound pressure level with the non-dimensional time and the Strouhal number. The units of the colour-scale are [dB]. The complex Morlet wavelet was used to compute the time-dependent spectrum.